

LETTER • **OPEN ACCESS**

Extreme wet events as important as extreme dry events in controlling spatial patterns of vegetation greenness anomalies

To cite this article: Caroline A Famiglietti *et al* 2021 *Environ. Res. Lett.* **16** 074014

View the [article online](#) for updates and enhancements.

You may also like

- [Probability of continued local-scale warming and extreme events during and after decarbonization](#)
Noah S Diffenbaugh, Elizabeth A Barnes and Patrick W Keys
- [Crop-specific exposure to extreme temperature and moisture for the globe for the last half century](#)
Nicole D Jackson, Megan Konar, Peter Debaere *et al.*
- [Likelihood of concurrent climate extremes and variations over China](#)
Ping Zhou and Zhiyong Liu



The Breath Biopsy® Guide
Fourth edition

FREE

DOWNLOAD THE FREE E-BOOK

BREATH BIOPSY

OWLSTONE MEDICAL

ENVIRONMENTAL RESEARCH
LETTERS

LETTER

Extreme wet events as important as extreme dry events in
controlling spatial patterns of vegetation greenness anomalies

OPEN ACCESS

RECEIVED

16 December 2020

REVISED

13 April 2021

ACCEPTED FOR PUBLICATION

28 April 2021

PUBLISHED

29 June 2021

Original content from
this work may be used
under the terms of the
[Creative Commons
Attribution 4.0 licence](#).

Any further distribution
of this work must
maintain attribution to
the author(s) and the title
of the work, journal
citation and DOI.

Caroline A Famiglietti^{1,*} , Anna M Michalak^{1,2} and Alexandra G Konings¹¹ Department of Earth System Science, Stanford University, Stanford, CA, United States of America² Department of Global Ecology, Carnegie Institution for Science, Stanford, CA, United States of America

* Author to whom any correspondence should be addressed.

E-mail: cfamigli@stanford.edu**Keywords:** extreme hydrological events, extreme wet events, terrestrial carbon uptake, climate changeSupplementary material for this article is available [online](#)**Abstract**

Understanding plant responses to hydrological extremes is critical for projections of the future terrestrial carbon uptake, but much more is known about the impacts of drought than of extreme wet conditions. However, the latter may control ecosystem-scale photosynthesis more strongly than the former in certain regions. Here we take a data-driven, location-based approach to evaluate where wet and dry extremes most affect photosynthesis. By comparing the sensitivity of vegetation greenness during extreme wetness to that during extreme dryness over a 34 year record, we find that regions where the impact of wet extremes dominates are nearly as common as regions where drought impacts dominate. We also demonstrate that the responses of wet-sensitive regions are not uniform and are instead controlled by multiple, often interacting, mechanisms. Given predicted increases in the frequency and intensity of extreme hydrological events with climate change, the consequences of extreme wet conditions on local and global carbon cycling will likely be amplified in future decades.

1. Introduction

Terrestrial carbon uptake by photosynthesis is strongly influenced by climate (Friedlingstein *et al* 2006) and its extremes (Reichstein *et al* 2013). As the climate warms, the hydrological cycle is intensifying (Trenberth 2011), yielding shifts in the regimes of extreme dry and extreme wet events (Seneviratne *et al* 2012). Droughts are expected to become more intense, spatially extensive, and temporally persistent (Trenberth *et al* 2014), while an enhancement of extreme wet precipitation has also been both projected (Fischer *et al* 2013) and observed (Donat *et al* 2016) on continental to global scales. To reduce uncertainties in future projections of the carbon cycle (Friedlingstein *et al* 2013), a robust understanding of the feedbacks between extreme hydrological events and terrestrial carbon uptake is crucial.

Because of this, the effects of droughts on growth and photosynthesis have been studied extensively (e.g. Farooq *et al* 2012, Schwalm *et al* 2017, Xu *et al* 2019). However, responses by vegetation to extreme wet events are poorly understood by comparison.

One possible contributor to this knowledge gap is the fact that, when globally averaged across the land surface, the impacts of extreme dry events on productivity have been shown to dominate those of extreme wet events (Zscheischler *et al* 2014). Such globally integrated values, however, may not fully capture the spectrum of relative impacts possible at any given location. Droughts are significantly more spatially coherent and less temporally transient than heavy rainfall events, which may contribute to the greater global impact of the former, regardless of which extreme is more influential in individual regions.

Overall, whether vegetation in any particular place is more sensitive to extreme wet events than to extreme dry events remains unclear. This is a crucial distinction because changes in the behavior of extreme hydrological events are also projected to vary regionally (albeit with high uncertainty (Trenberth 2011)). That is, different regions will experience different trends in extreme precipitation, with some getting wetter and others drier. If hotspots of sensitivity to extreme wet events exist now, their future consequences on local and global carbon cycling could be

even more pronounced. Furthermore, understanding how the vulnerability of different regions to hydrological extremes varies may impact conservation or management priorities.

Beyond the importance of extreme wet events on sub-global scales, even the dominant sign of the photosynthesis response under extreme wetness is poorly quantified across the broader land surface. Significant heterogeneity in both sign and magnitude of the vegetation response to extreme wetness has been observed at ecosystem scales (Heisler-White *et al* 2008, Knapp *et al* 2008), indicating its dependence on locally- and regionally-specific factors. A multitude of processes can impact the response of vegetation to extreme wet conditions. Some such mechanisms may cause photosynthesis to increase (e.g. by alleviating a moisture limitation or by mitigating heat-related stresses (Li *et al* 2019)), while others may induce negative effects (e.g. associated with the consequences of partial to complete flooding (Bailey-Serres and Voesenek 2008, Garssen *et al* 2015)). Because a bottom-up study tracing each process to its impact on carbon uptake is not feasible given the data that is currently available, here we take a top-down approach by first quantifying vegetation responses during extreme wet conditions and then inferring likely mechanisms that explain the observed patterns.

This paper investigates regional variations in the relative impacts of extreme wet events and extreme dry events on vegetation. To do so, average vegetation greenness anomalies (relative to the local climatology) during periods of extremely high moisture were compared to those during periods of extremely low moisture by leveraging 34 years of satellite normalized difference vegetation index (NDVI) data from the Global Inventory Monitoring and Modeling System (GIMMS) alongside combined active and passive soil moisture observations from the European Space Agency Climate Change Initiative (ESA CCI) (see section 2). Although NDVI is a direct measure of spectral reflectance, not photosynthesis (Tucker 1978), it is used here because of its long temporal record, observational nature, and global spatial coverage.

Specifically, in this paper we seek to answer the following questions. (a) Across the vegetated land surface, where is greenness more sensitive to extreme wet events than it is to extreme dry events? (b) What controls the sign of the resulting greenness change during extreme wet events?

2. Methods

2.1. Data selection and processing

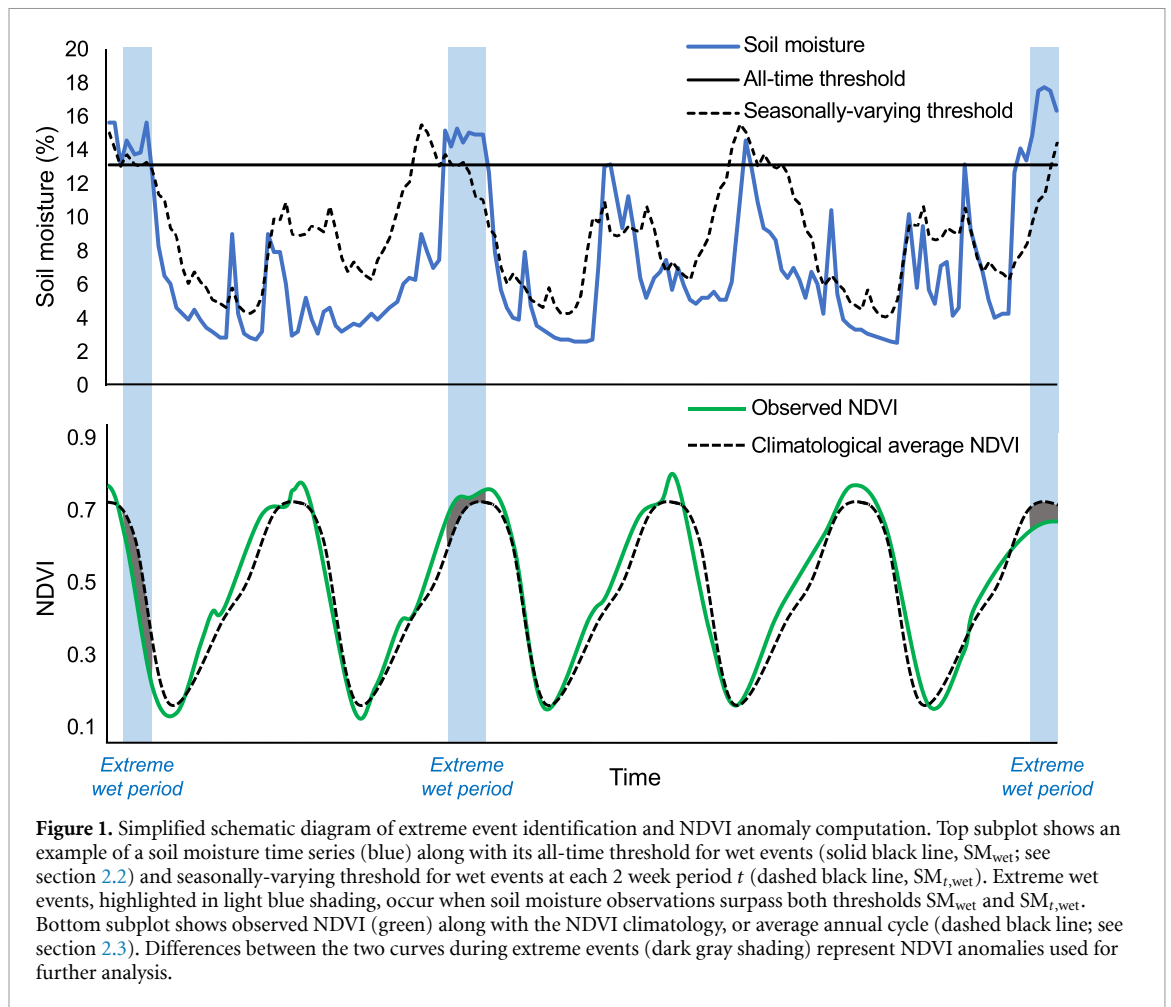
Two datasets derived from satellite remote sensing were used to represent vegetation productivity and moisture conditions. These datasets were selected on the basis of their (a) long temporal

records (i.e. >30 years), (b) moderate-to-high spatial resolutions, (c) global coverage, and (d) observational nature (i.e. absence of assumptions about vegetation behavior embedded in the datasets).

We used the GIMMS NDVI third generation data product as a proxy for vegetation productivity. The dataset is derived from Advanced Very High Resolution Radiometer (AVHRR) imagery (Tucker *et al* 2005, Pinzon and Tucker 2014) and spans the period July 1981–December 2015 at 1/12° spatial resolution and bimonthly (15 d) composite temporal resolution. While NDVI is not a direct measure of photosynthesis, its dynamics capture changes in vegetation greenness (Tucker 1978), which are assumed to indicate variations in productivity on a biweekly timescale.

Next, we used soil moisture data—specifically, the ESA CCI combined soil moisture product v04.4 (Dorigo *et al* 2017)—to describe moisture conditions. The combined product incorporates both active scatterometer data and passive radiometer data from a variety of sensors. It spans the period November 1978–June 2018 at 0.25° spatial resolution with daily observations, although the observational density of the product varies depending on the number of sensors that are operational at any point in time. This temporal frequency is a key advantage of the CCI soil moisture product relative to monthly metrics such as the standardized precipitation–evapotranspiration index (Vicente-Serrano *et al* 2010), particularly in the context of extreme wet events, which are often shorter than extreme dry events. Although soil moisture observed by microwave remote sensing represents near-surface conditions rather than the entire root zone, which would be more informative of the moisture conditions influencing vegetation, observational datasets of root-zone soil moisture are not available at the global scale. The use of an observational dataset, in contrast to model-based products (e.g. those from the Global Land Data Assimilation System (GLDAS; Rodell *et al* 2004), ensures that the effects of highly variable processes like infiltration on soil moisture are correctly accounted for. Consistent with other studies (e.g. Li *et al* 2019, Liu *et al* 2020, Orth *et al* 2020), we considered surface soil moisture informative because it tends to be well correlated with that in deeper layers (McColl *et al* 2017). Furthermore, because extreme wet events are unlikely to occur in deeper layers without also being reflected in the surface, our approach is more likely to identify false positives rather than false negatives and is thus conservative with respect to the impact of wet extremes.

To harmonize the soil moisture and NDVI datasets, we selected the period July 1981–December 2015 for analysis, linearly resampled the NDVI data to 0.25° spatial resolution and computed biweekly soil moisture averages for comparison with NDVI. This



averaging procedure also led to smoothing of the noise in the soil moisture observations.

Vegetation responses to periods of extreme moisture were also compared to several climatic and vegetation factors. These variables included air temperature and shortwave radiation from the 5th generation European Centre for Medium-Range Weather Forecasts atmospheric reanalysis of the global climate (ERA5; Hersbach *et al* 2020); potential evapotranspiration (PET) and rainfall rate from GLDAS; an index of aridity (the ratio of precipitation to PET) based on WorldClim 2.0 data (Trabucco and Zomer 2019); and leaf area index (LAI) climatology from GIMMS (Mao and Yan 2019). Vapor pressure deficit (VPD) was computed using the Roche–Magnus equation.

2.2. Isolating extreme moisture events

We implemented two concurrent thresholds to isolate extreme soil moisture events at each pixel: (a) an ‘all-time’ threshold ensuring that events are extreme relative to the entire record of observation; and (b) a seasonally-varying threshold ensuring they are such relative to their date of occurrence. The soil moisture time series shown in figure 1 demonstrates this identification procedure, using wet extremes as an example.

To compute the all-time thresholds, a percentile-based cutoff for extreme dry events (SM_{dry}) and one for extreme wet events (SM_{wet}) were determined for each pixel using its full soil moisture time series. SM_{dry} was equivalent to the soil moisture value at a chosen percentile p and SM_{wet} was equivalent to that at $100 - p$. In the main figures of this paper, p was set to 15 to ensure a sufficient sample size, although we tested the effects of several increasingly extreme values of p in a sensitivity analysis. Figure S1 (available online at stacks.iop.org/ERL/16/074014/mmedia) shows that our main results remain consistent across several choices of p .

To ensure that events identified as extreme based on SM_{dry} and SM_{wet} were not biased towards that pixel’s driest and wettest seasons, we further imposed seasonally-varying thresholds to determine whether they were also extreme relative to their time of year. We computed dry-event and wet-event seasonally-varying thresholds for each 2 week period (t) of the year by assuming a Gaussian distribution of the inter-annual values of soil moisture. This approach differs slightly from that used to calculate the all-time thresholds because of the reduced number of observations available when only a certain time of year is considered. The seasonally-varying threshold for dry

events ($SM_{t,dry}$) and that for wet events ($SM_{t,wet}$) were calculated as:

$$SM_{t,dry} = \mu_t - |z| \cdot \sigma_t$$

$$SM_{t,wet} = \mu_t + |z| \cdot \sigma_t$$

where μ_t is the climatological average soil moisture at time t , z is the z -score corresponding to percentile p (e.g. $|z| = 1.04$ for $p = 15$), and σ_t is the standard deviation of observations yielding the climatology at timestep t .

To summarize, events identified as extreme using the all-time method were ultimately accepted only if they were also classified as such using the seasonally-varying method. That is, all soil moisture observations that fell below both SM_{dry} and $SM_{t,dry}$ were identified as extreme dry events and included in our analysis, and all that exceeded both SM_{wet} and $SM_{t,wet}$ were classified as extreme wet events (figure 1) and included. We note that regions for which soil moisture data were unavailable were necessarily excluded from the analysis.

We repeated the same extreme event classification procedure for both the radiation and temperature data. In order to ensure the events considered primarily reflected responses to hydrological rather than other climatic factors, any soil moisture extreme that co-occurred with a temperature or radiation extreme (22.9% of dry extremes and 19.0% of wet extremes) was removed from the analysis.

2.3. Identifying growing seasons from NDVI data

To identify growing seasons from the NDVI time series at each pixel, we first computed the NDVI climatology by averaging observations for each 2 week period across all years. This climatology represents the pixel's average annual cycle of NDVI. For each year, we identified the growing season as those values exceeding $(NDVI_{max} - NDVI_{min}) / 2$, where $NDVI_{max}$ is the peak and $NDVI_{min}$ is the minimum of the average seasonal cycle, respectively. This approach is similar to previous efforts (White *et al* 1997, Vrieling *et al* 2013). Any soil moisture extreme that was identified but did not occur in a pixel's growing season was removed from the analysis.

2.4. Computing average NDVI anomalies during extreme moisture events

For every pixel, we computed the average NDVI anomaly during extreme wet events ($NDVI_W$) and the average NDVI anomaly during extreme dry events ($NDVI_D$) in the following way:

$$NDVI_W = \frac{\sum_{i=0}^{n_W} (NDVI_i - \overline{NDVI}_i)}{n_W}$$

$$NDVI_D = \frac{\sum_{j=0}^{n_D} (NDVI_j - \overline{NDVI}_j)}{n_D}$$

where i are the timesteps during which a total of n_W extreme wet events occurred, j are the timesteps during which a total of n_D extreme dry events occurred, $NDVI_i$ and $NDVI_j$ are the NDVI observations at times i and j , and \overline{NDVI}_i and \overline{NDVI}_j are the NDVI climatological averages corresponding to times i and j . Figure 1 shows how the extreme event identification procedure maps to NDVI anomalies.

$NDVI_W$ and $NDVI_D$ were tested for statistical significance (student's t -test, $p < 0.05$) against all differences between observations and climatology over the entire record. Only significant values were included in the analysis.

2.5. Statistical comparison of distributions

We used the two-sample Kolmogorov–Smirnov test, or K–S test, to evaluate the equality of continuous climate and vegetation-related distributions (in particular, those tested as potential explanatory factors differentiating $NDVI_W$ from $NDVI_D$; see last paragraph of section 2.1). The test is used to assess whether two samples are statistically indistinguishable from one another (i.e. whether they were drawn from the same distribution). It returns the Kolmogorov–Smirnov statistic, which is the maximum distance between the empirical cumulative distribution functions of the two samples, as well as a p -value used for significance testing. No normality assumptions are required for its implementation. Theoretically, two dissimilar distributions will be characterized by a large Kolmogorov–Smirnov statistic, and two similar ones will have a small Kolmogorov–Smirnov statistic (figure S2). Here, results are included only for Kolmogorov–Smirnov statistics that were significant ($p < 0.05$).

3. Results

3.1. Regional-scale sensitivity to extreme wet and extreme dry events

Strong sensitivity hotspots exist for both wet and dry extremes, indicating regions for which vegetation greenness anomalies are strongly coupled to extreme hydrological events (figures 2(a) and (b)). High-magnitude sensitivities to both extreme wet events and extreme dry events appear in northeastern Australia and southern Africa, while many northern boreal regions are significantly sensitive only to the former and parts of India are only to the latter.

For 11.6% of the vegetated global land surface, average NDVI anomalies are larger in magnitude during extreme wet events than they are during extreme dry events (i.e. the absolute value of $NDVI_W$ exceeded that of $NDVI_D$), indicating a greater overall vegetation sensitivity to wetness than to dryness in those regions (figure 2(c)). This fraction is only slightly less than that for which NDVI is more sensitive to extreme dry events (14.4%; the remaining 74.0% is

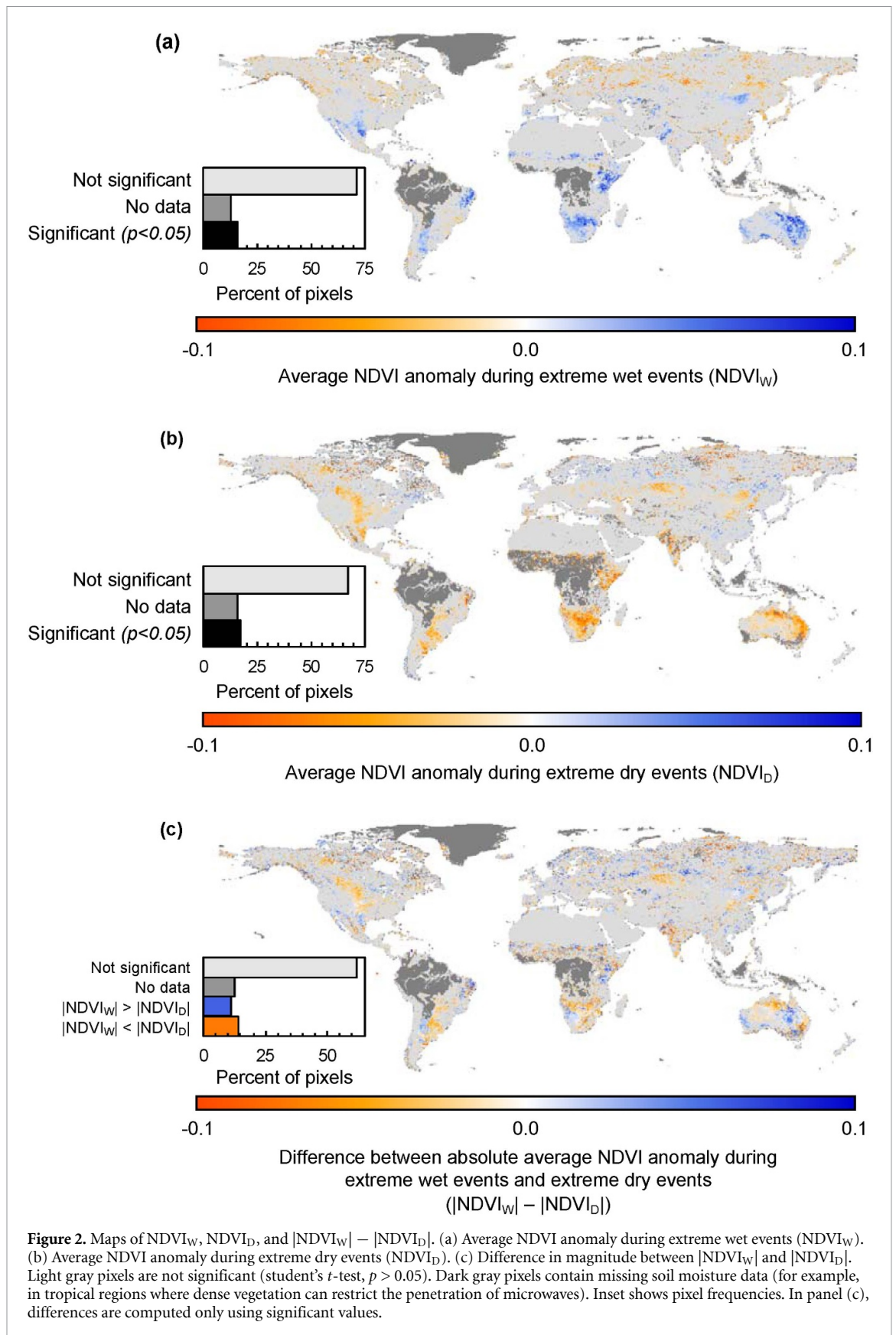


Figure 2. Maps of $NDVI_W$, $NDVI_D$, and $|NDVI_W| - |NDVI_D|$. (a) Average NDVI anomaly during extreme wet events ($NDVI_W$). (b) Average NDVI anomaly during extreme dry events ($NDVI_D$). (c) Difference in magnitude between $|NDVI_W|$ and $|NDVI_D|$. Light gray pixels are not significant (student's t -test, $p > 0.05$). Dark gray pixels contain missing soil moisture data (for example, in tropical regions where dense vegetation can restrict the penetration of microwaves). Inset shows pixel frequencies. In panel (c), differences are computed only using significant values.

either not statistically significant or contains missing data (see inset of figure 2(c)). The near equivalence of these two fractions holds even when varying the soil moisture threshold used for identifying

extreme events (figure S1) as well as when omitting agricultural regions from the analysis (figure S3), since their greenness responses may be skewed by irrigation use. Overall, this surprising result suggests

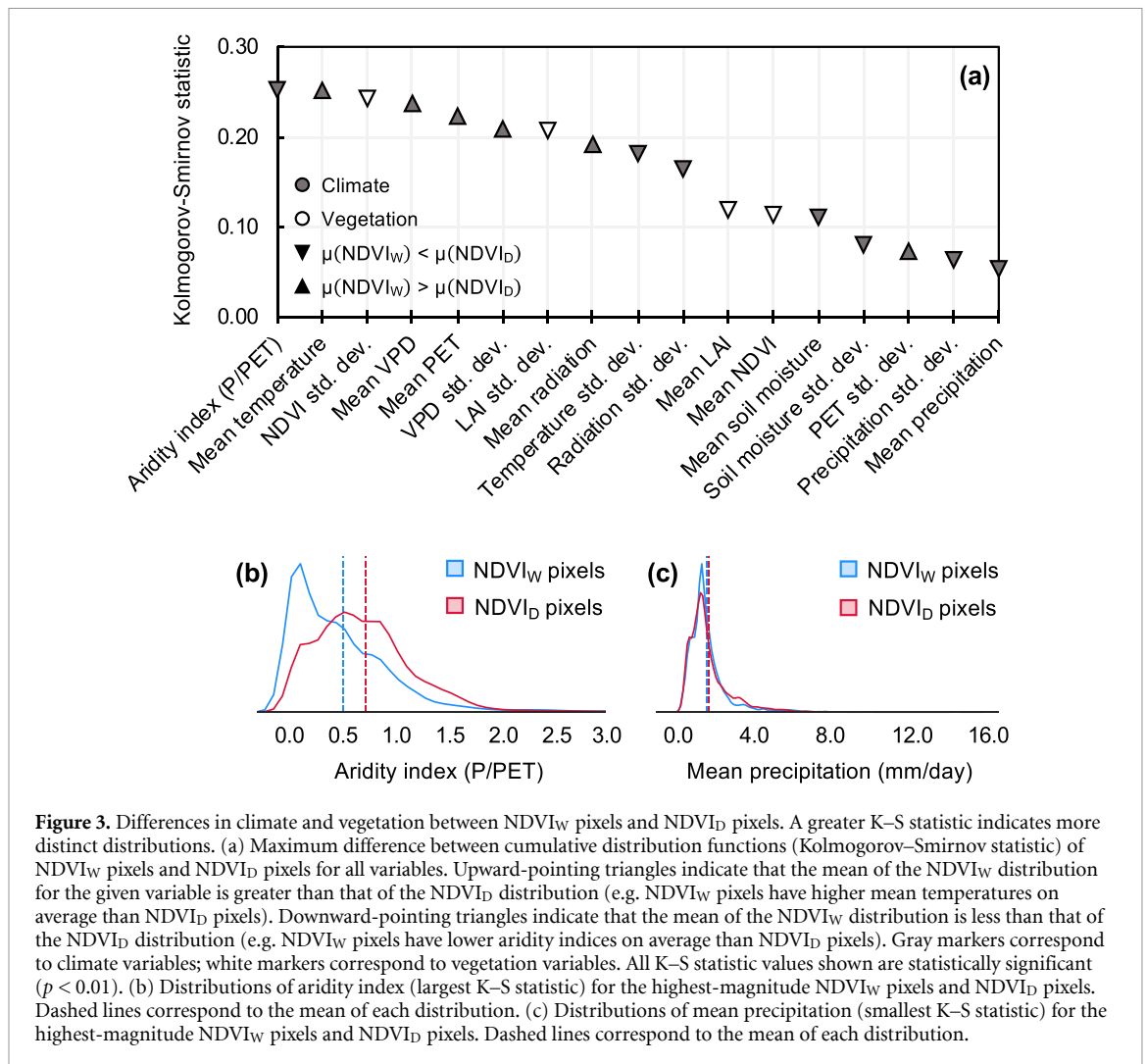


Figure 3. Differences in climate and vegetation between NDVI_W pixels and NDVI_D pixels. A greater K–S statistic indicates more distinct distributions. (a) Maximum difference between cumulative distribution functions (Kolmogorov–Smirnov statistic) of NDVI_W pixels and NDVI_D pixels for all variables. Upward-pointing triangles indicate that the mean of the NDVI_W distribution for the given variable is greater than that of the NDVI_D distribution (e.g. NDVI_W pixels have higher mean temperatures on average than NDVI_D pixels). Downward-pointing triangles indicate that the mean of the NDVI_W distribution is less than that of the NDVI_D distribution (e.g. NDVI_W pixels have lower aridity indices on average than NDVI_D pixels). Gray markers correspond to climate variables; white markers correspond to vegetation variables. All K–S statistic values shown are statistically significant ($p < 0.01$). (b) Distributions of aridity index (largest K–S statistic) for the highest-magnitude NDVI_W pixels and NDVI_D pixels. Dashed lines correspond to the mean of each distribution. (c) Distributions of mean precipitation (smallest K–S statistic) for the highest-magnitude NDVI_W pixels and NDVI_D pixels. Dashed lines correspond to the mean of each distribution.

that the spatial extents of the two types of vegetation sensitivities are comparable. That is, when sampling any specific location, it is almost as common for greenness to be more sensitive to wet extremes than to dry extremes.

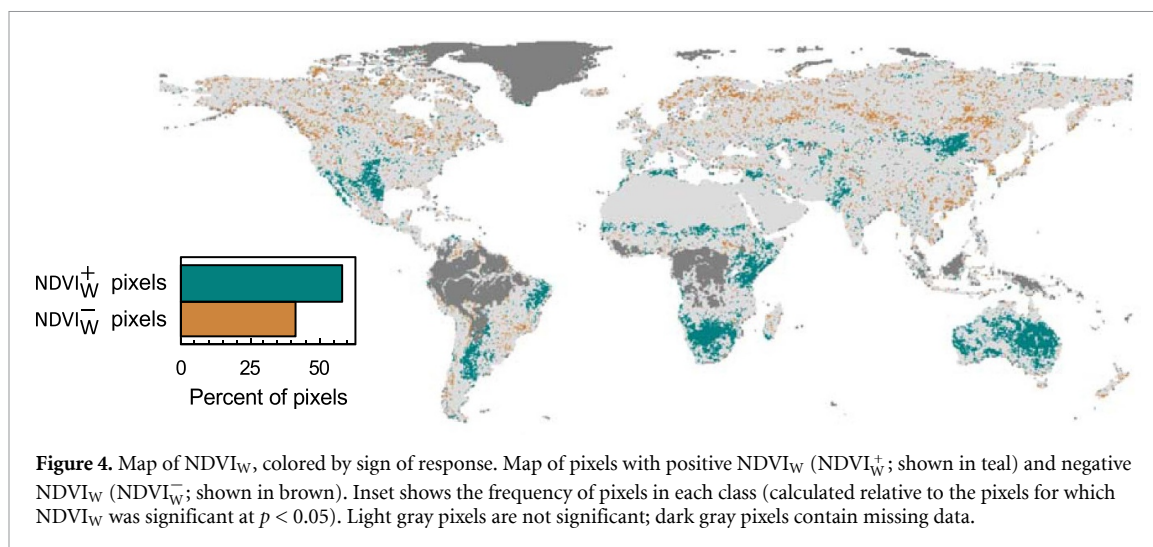
Measures of average atmospheric moisture demand conditions, including mean PET, mean VPD, and the ratio of precipitation to PET (a common index of aridity), most strongly differentiate the class of pixels with high-magnitude NDVI_W from those with high-magnitude NDVI_D (figure 3(a)). Specifically, pixels with the greatest sensitivity to wet events are characterized by lower aridity indices (figure 3(b); indicating PET far greater than the supply of water by precipitation), higher mean PET (suggestive of a larger moisture gradient, and thus a greater capacity for hydrologic exchange from the land to the atmosphere), greater VPD, higher radiation, and higher temperature than the most drought-sensitive pixels (figure S4). Notably, neither mean precipitation itself, nor precipitation variability, are strong differentiators between the two types of pixels (figure 3(c)), suggesting that moisture demand exerts a greater control than moisture availability over the spatial distribution of vegetation sensitivity

to hydrological extremes. These climate-based distinctions also dominate differences in average land cover in their explanatory power. Mean LAI and mean NDVI were relatively similar between the two types of pixels, indicating representation from a broad range of vegetation covers, although pixels with lower temporal variability in NDVI tend to be more sensitive to wet extremes. Taken together, these results highlight the impacts of extreme hydrological events that oppose a region's dominant aridity regime, irrespective of its mean vegetation state, on greenness anomalies. Amid projections of enhanced wet extremes, they also draw attention to the future role of arid and semi-arid ecosystems in the global carbon cycle (Poulter *et al* 2014, Ahlström *et al* 2015).

3.2. Sign of greenness change during extreme wet events

3.2.1. Spatial patterns

In 41.4% of pixels with a statistically significant response to extreme wetness, NDVI typically declines relative to its climatology during periods of extremely high moisture, while NDVI typically increases during these periods in 58.6% of pixels (figure 4). Note that for this analysis, we separated the subset of vegetated



pixels for which $NDVI_W$ is positive (hereafter referred to as $NDVI_W^+$) from that for which it is negative (hereafter referred to as $NDVI_W^-$) under extremely high moisture. There are regionally coherent patterns in the occurrence of $NDVI_W^+$ and $NDVI_W^-$ pixels; regions like eastern Australia and southern Africa are dominated by $NDVI_W^+$ pixels, while $NDVI_W^-$ pixels account for large swaths of the northern high latitudes (figure 4). Most $NDVI_W^+$ pixels are arid or semi-arid regions; they tend to be warmer and drier than $NDVI_W^-$ pixels (figure S5), highlighting the ability of moisture-limited regions to translate even the most extreme additions of moisture over the 34 years record into increased greenness.

3.2.2. Event-scale controls on reduced greenness

While the analysis into spatial patterns largely explains the occurrence of positive NDVI anomalies during extreme wetness (i.e. they are predominantly linked to moisture-limited regions), the mechanisms contributing to reduced greenness during extreme wet conditions are more difficult to elucidate. To better understand such negative responses, we further focused on the timescale of individual extreme events. Though this approach inevitably includes significant uncertainties because our study uses observational data rather than controlled experiments, we identified two emergent patterns that may be interpreted as promising avenues for further research.

First, negative NDVI anomalies during extreme wet events tend to occur during growing seasons for which NDVI is already lower than average (figure S6(a)), suggesting that vegetation greenness was already depressed relative to the local climatology before the extreme event took place. This suggests that the occurrence of the extreme event, and the response by vegetation to it, may not be independent from the preceding climate conditions that caused the low-greenness observation. The magnitude of the NDVI

anomaly is still greater—on average—during the wet extreme than before it, implying that this form of short-term memory influences the anomaly response but is not the sole cause.

Additionally, in some pixels, there is some evidence to support the hypothesis that a negative greenness response may be explained by excessive soil saturation, or waterlogging. Waterlogging can cause the soil to become so saturated that the plant cannot access enough oxygen to adequately respire (known as soil hypoxia). Soil hypoxia can decrease stomatal conductance and root hydraulic conductivity, among other negative impacts on plant growth and soil properties (Parent *et al* 2008). It is difficult to explicitly quantify the degree to which waterlogging occurs at a global scale, however, because it is not known how the soil moisture levels necessary to induce hypoxia vary across the globe. Furthermore, biases in soil moisture observations (Dorigo *et al* 2015) and global soil texture databases, which are likely a first order control on soil moisture levels required for saturation, would further complicate such an analysis.

As an indirect proxy for waterlogging, we considered different classes of extreme soil wetness, stratified based on the local soil moisture distribution. Across all pixels, wet extremes are distributed non-normally: that is, extremes occurring above that pixel's 95th percentile are more common than extremes occurring between its 90th and 95th percentile, which in turn are more common than those in the 85th-to-90th percentile class. Critically, however, it is more likely for events occurring at the highest soil moisture percentiles to yield decreased NDVI than to yield increased NDVI (table S1). It is therefore possible that a higher fraction of the wet extremes associated with reduced greenness may occur during waterlogged conditions. The possible role of waterlogging warrants further study as possible controls on the sign of the response by vegetation to extreme wetness.

4. Discussion

More attention to both types of extreme hydrological events—droughts as well as heavy precipitation—is needed to understand their impacts on vegetation now and in future decades. While which impact is dominant varies greatly across the land surface (figure 2(c)), many places exhibit significant sensitivities to both extreme wet and dry events (figures 2(a) and (b)). The carbon balance of such regions is therefore a function of multiple, dynamically evolving extreme event regimes. Coupled with the finding that the spatial extents of the two types of sensitivities are comparable, this contrasts with the significantly larger focus in the literature on dry, rather than wet, events (e.g. Farooq *et al* 2012, Schwalm *et al* 2017, Xu *et al* 2019).

The global distribution of NDVI_W^+ and NDVI_W^- pixels demonstrated here aligns with prior work in grasslands suggesting that the response by terrestrial ecosystems to extreme rainfall events is highly nonlinear (e.g. Heisler-White *et al* 2008, Knapp *et al* 2008). However, our findings broaden the scope of such work in two key ways. First, our data-driven study indicates that bidirectional productivity responses (i.e. that productivity can either increase or decrease during extreme wetness) persist across far larger spatial and temporal scales than previously captured by field studies, and across biome types. Specifically, they persist across the scales relevant to informing and improving land surface models (which have been shown, for instance, to misrepresent the growth legacy effects of extreme wetness in many forests (Jiang *et al* 2019)).

Second, we observed that controls on the sign of the greenness response under extreme wetness are also more complex than previously demonstrated under experimental conditions. While the observed sensitivity of arid regions is generally linked to average atmospheric moisture demand (figure 3), other factors—beyond mean climate conditions—may interact to impact the overall response by vegetation to extreme wetness in cases where greenness was ultimately reduced.

For instance, we took steps to isolate the impacts of extreme wet events on greenness (e.g. by only considering events that did not co-occur with radiation or temperature extremes; see section 2), but still found an inextricable effect of prior climate on both the magnitude and sensitivity of the vegetation response (figure S6). While previous work has focused on ‘legacy effects’ of extreme hydrological events on carbon fluxes (i.e. given an extreme event, how will vegetation respond in seasons to follow?) (e.g. Anderegg *et al* 2015, Jiang *et al* 2019, Gao *et al* 2020 at interannual timescales; or Schwalm *et al* 2017, Kolus *et al* 2019 at monthly timescales), we also found evidence of the inverse causality (a given prior vegetation anomaly exerts some

control over its response to a later extreme wet event).

In particular, below-average carbon uptake—which may result from shifts in average temperature, cloud cover, or precipitation patterns diminishing photosynthetic rates—appears to affect the further depression of greenness during subsequent extreme wet conditions. A similar dynamic was identified by Randazzo *et al* (2020) in the context of linking synoptic meteorology to North American ecosystem carbon exchange at the site scale. It remains unclear, however, which prior climate conditions—and over what timescales—are most significant in affecting vegetation responses to later extreme wet events.

An additional limitation in understanding the tradeoffs between mechanisms controlling reduced greenness under extreme rainfall is the challenge of predicting where and when soil waterlogging, along with possible hypoxic or anoxic conditions, will occur. The occurrence of waterlogging and its consequences on plant functioning depend on both dynamic and static factors (including local and regional hydrology, soil texture, and slope position), and because of temporal gaps in soil moisture data and uncertainty in soil properties, it is often difficult to assess the prevalence of waterlogging directly at any given location.

Some evidence points to high-latitude regions as especially susceptible to over-saturated conditions. In particular, the fact that we observed a greater likelihood for NDVI-suppressing events in the northern high-latitudes (figure 4) is sensible given (a) the region’s higher long-term average soil moisture relative to the consistently drier mid-latitudes (McColl *et al* 2017), (b) shallow groundwater tables in the region (Fan *et al* 2013), and (c) observations that in some of the most extreme northern ecosystems, melting snow, ice, and permafrost can further increase soil saturation (Turetsky *et al* 2007). Still, the properties of waterlogging (e.g. duration, time of year, climatological history) that most influence its effect on productivity, and how the likelihood of waterlogging varies through space and time across the land surface, remain unclear.

5. Conclusions

Using 34 years of satellite data, we found that regions more sensitive to extreme wet events than to extreme dry events are more prevalent than previously recognized. The greenness responses of those regions are not uniform; they are functions of multiple, often interacting, mechanisms (e.g. atmospheric moisture demand, average and preceding climate conditions, etc). Although regions where extreme wet events significantly affect vegetation greenness are widespread, the plant response to them remains poorly understood. In particular, the processes that control negative productivity responses to extreme wetness

have not been studied in depth, and the relative roles and interactions of factors such as soil properties (Li *et al* 2019), the duration of soil hypoxia (Horchani *et al* 2008), or wind damage (Gardiner *et al* 2016) are not known. Similarly, while pre-event conditions influence the response to wet extremes (figure S6), the magnitude, pathways, and prevalence of that influence likely differ from region to region or event to event. Additionally, although events for which extreme soil moisture conditions coincide with extremes in temperature or radiation were excluded from this study, extreme wetness may also play an important role in regulating vegetation productivity during compound or co-occurring extremes (Zscheischler and Seneviratne 2017, Zscheischler *et al* 2018).

To parse the dynamics controlling the response to extreme wetness, future studies at higher spatiotemporal resolutions than the long-term global assessment here may benefit from recent advances in remote sensing of photosynthesis such as solar-induced fluorescence (Guanter *et al* 2014) or the near-infrared reflectance of vegetation (Badgley *et al* 2017), which more directly relate to carbon uptake than NDVI does. The increased study of extreme wet events is likely to improve forecasts of vegetation productivity, with further benefits for conservation, resource management, timber logging, and the quantification of ecosystem services.

Overall, the impacts of extreme hydrological events on carbon uptake will likely strengthen in a changing climate characterized by increasingly frequent and intense wet and dry periods. While it is possible that in some regions, the cumulative effects of droughts and extreme wet events will compensate on sufficiently long timescales (i.e. from year to year, reduced productivity during the former may be offset by increases during the latter), the prevalence of bidirectional responses to extreme wetness identified here, and the conditionality of its sign on a suite of interacting factors, complicate the likelihood of this outcome.

Data availability statement

The data that support the findings of this study are available upon reasonable request from the authors.

Acknowledgments

C A F, A M M, and A G K designed research. C A F processed and analyzed data. C A F, A M M, and A G K interpreted the results. C A F wrote the paper with support from A M M and A G K. All authors reviewed drafts of the manuscript. Feedback from three anonymous reviewers contributed to significant improvements in the manuscript's clarity.

Conflicts of interest

The authors declare that they have no competing interests.

Funding

CAF was funded by a Stanford Graduate Fellowship. A G K was funded by N O A A Grant NA17OAR4310127.

ORCID iD

Caroline A Famiglietti  <https://orcid.org/0000-0002-6073-0457>

References

- Ahlström A, Raupach M R, Schurgers G, Smith B, Arneth A, Jung M and Zeng N 2015 The dominant role of semi-arid ecosystems in the trend and variability of the land CO₂ sink *Science* **348** 895 LP–899
- Anderegg W R L, Schwalm C, Biondi F, Camarero J J, Koch G, Litvak M and Pacala S 2015 Pervasive drought legacies in forest ecosystems and their implications for carbon cycle models *Science* **349** 528 LP–532
- Badgley G, Field C B and Berry J A 2017 Canopy near-infrared reflectance and terrestrial photosynthesis *Sci. Adv.* **3** e1602244
- Bailey-Serres J and Voesenek L A C J 2008 Flooding stress: acclimations and genetic diversity *Annu. Rev. Plant Biol.* **59** 313–39
- Donat M G, Lowry A L, Alexander L V, O’Gorman P A and Maher N 2016 More extreme precipitation in the world’s dry and wet regions *Nat. Clim. Change* **6** 508
- Dorigo W A, Gruber A, de Jeu R A M, Wagner W, Stacke T, Loew A and Parinussa R M 2015 Evaluation of the ESA CCI soil moisture product using ground-based observations *Remote Sens. Environ.* **162** 380–95
- Dorigo W A, Wagner W, Albergel C, Albrecht F, Balsamo G, Brocca L and Lecomte P 2017 ESA CCI soil moisture for improved earth system understanding: state-of-the art and future directions *Remote Sens. Environ.* **203** 185–215
- Fan Y, Li H and Miguez-Macho G 2013 Global patterns of groundwater table depth *Science* **339** 940 LP–943
- Farooq M, Hussain M, Wahid A and Siddique K H M 2012 Drought stress in plants: an overview *Plant Responses to Drought Stress* (Berlin: Springer) pp 1–33
- Fischer E M, Beyerle U and Knutti R 2013 Robust spatially aggregated projections of climate extremes *Nat. Clim. Change* **3** 1033–8
- Friedlingstein P, Cox P, Betts R, Bopp L, von Bloh W, Brovkin V and Zeng N 2006 Climate–carbon cycle feedback analysis: results from the C4MIP model intercomparison *J. Clim.* **19** 3337–53
- Friedlingstein P, Meinshausen M, Arora V K, Jones C D, Anav A, Liddicoat S K and Knutti R 2013 Uncertainties in CMIP5 climate projections due to carbon cycle feedbacks *J. Clim.* **27** 511–26
- Gao S, Zhou T, Yi C, Shi P, Fang W, Liu R and Julio Camarero J 2020 Asymmetric impacts of dryness and wetness on tree growth and forest coverage *Agric. For. Meteorol.* **288–289** 107980
- Gardiner B, Berry P and Moulia B 2016 Review: wind impacts on plant growth, mechanics and damage *Plant Sci.* **245** 94–118
- Garssen A G, Baatrup-Pedersen A, Voesenek L A C J, Verhoeven J T A and Soons M B 2015 Riparian plant community responses to increased flooding: a meta-analysis

- Glob. Change Biol.* **21** 2881–90
- Guanter L, Zhang Y, Jung M, Joiner J, Voigt M, Berry J A and Griffis T J 2014 Global and time-resolved monitoring of crop photosynthesis with chlorophyll fluorescence *Proc. Natl Acad. Sci.* **111** E1327–33
- Heisler-White J L, Knapp A K and Kelly E F 2008 Increasing precipitation event size increases aboveground net primary productivity in a semi-arid grassland *Oecologia* **158** 129–40
- Hersbach H, Bell B, Berrisford P, Hirahara S, Horányi A and Muñoz-Sabater J 2020 The ERA5 global reanalysis *Q. J. R. Meteorol. Soc.* **146** 1999–2049
- Horchani F, Aloui A, Brouquisse R and Aschi-Smiti S 2008 Physiological responses of tomato plants (*solanum lycopersicum*) as affected by root hypoxia *J. Agron. Crop Sci.* **194** 297–303
- Jiang P, Liu H, Piao S, Ciais P, Wu X, Yin Y and Wang H 2019 Enhanced growth after extreme wetness compensates for post-drought carbon loss in dry forests *Nat. Commun.* **10** 195
- Knapp A K, Beier C, Briske D D, Classen A T, Luo Y, Reichstein M and Weng E 2008 Consequences of more extreme precipitation regimes for terrestrial ecosystems *Bioscience* **58** 811–21
- Kolus H R, Huntzinger D N, Schwalm C R, Fisher J B, McKay N, Fang Y and Shi X 2019 Land carbon models underestimate the severity and duration of drought's impact on plant productivity *Sci. Rep.* **9** 2758
- Li Y, Guan K, Schnitkey G D, DeLucia E and Peng B 2019 Excessive rainfall leads to maize yield loss of a comparable magnitude to extreme drought in the United States *Glob. Change Biol.* **25** 2325–37
- Liu L, Gudmundsson L, Hauser M, Qin D, Li S and Seneviratne S I 2020 Soil moisture dominates dryness stress on ecosystem production globally *Nat. Commun.* **11** 4892
- Mao J and Yan B 2019 Global monthly mean leaf area index climatology, 1981–2015 ORNL distributed active archive center (<https://doi.org/10.3334/ORNLDACC/1653>)
- McColl K A, Alemohammad S H, Akbar R, Konings A G, Yueh S and Entekhabi D 2017 The global distribution and dynamics of surface soil moisture *Nat. Geosci.* **10** 100–4
- Orth R, Destouni G, Jung M and Reichstein M 2020 Large-scale biospheric drought response intensifies linearly with drought duration in arid regions *Biogeosciences* **17** 2647–56
- Parent C, Capelli N, Berger A, Crevêcoeur M and Dat J 2008 An overview of plant responses to soil waterlogging *Plant Stress* **2** 20–7
- Pinzon E J and Tucker J C 2014 A non-stationary 1981–2012 AVHRR NDVI3g time series *Remote Sens.* **6** 929–60
- Poulter B, Frank D, Ciais P, Myneni R B, Andela N, Bi J and van der Werf G R 2014 Contribution of semi-arid ecosystems to interannual variability of the global carbon cycle *Nature* **509** 600
- Randazzo N A, Michalak A M and Desai A R 2020 Synoptic meteorology explains temperate forest carbon uptake *J. Geophys. Res.* **125** e2019JG005476
- Reichstein M, Bahn M, Ciais P, Frank D, Mahecha M D, Seneviratne S I and Wattenbach M 2013 Climate extremes and the carbon cycle *Nature* **500** 287
- Rodell M, Houser P R, Jambor U, Gottschalck J, Mitchell K, Meng C-J and Toll D 2004 The global land data assimilation system *Bull. Am. Meteorol. Soc.* **85** 381–94
- Schwalm C R, Anderegg W R L, Michalak A M, Fisher J B, Biondi F, Koch G and Tian H 2017 Global patterns of drought recovery *Nature* **548** 202
- Seneviratne S I, Nicholls N, Easterling D, Goodess C M, Kanae S, Kossin J and Zwiers F W 2012 Changes in climate extremes and their impacts on the natural physical environment eds C B Field, Q Dahe, T F Stocker and V Barros *Managing the Risks of Extreme Events and Disasters to Advance Climate Change Adaptation: Special Report of the Intergovernmental Panel on Climate Change* (Cambridge: Cambridge University Press) pp 109–230
- Trabucco A and Zomer R 2019 Global aridity index and potential evapotranspiration (ET0) climate database v2 18 January (<https://doi.org/10.6084/m9.figshare.7504448.v3>)
- Trenberth K E 2011 Changes in precipitation with climate change *Clim. Res.* **47** 123–38
- Trenberth K E, Dai A, van der Schrier G, Jones P D, Briffa K R and Sheffield J 2014 Global warming and changes in drought *Nat. Clim. Change* **4** 17–22
- Tucker C J 1978 Red and photographic infrared linear combinations for monitoring vegetation
- Tucker C J, Pinzon J E, Brown M E, Slayback D A, Pak E W, Mahoney R and El Saleous N 2005 An extended AVHRR 8 km NDVI dataset compatible with MODIS and SPOT vegetation NDVI data *Int. J. Remote Sens.* **26** 4485–98
- Turetsky M, Wieder R, Vitt D, Evans R and Scott K 2007 The disappearance of relict permafrost in boreal North America: effects on peatland carbon storage and fluxes *Glob. Change Biol.* **13** 1922–34
- Vicente-Serrano S M, Beguería S and López-Moreno J I 2010 A multiscalar drought index sensitive to global warming: the standardized precipitation evapotranspiration index *J. Clim.* **23** 1696–718
- Vrieling A, de Leeuw J and Said M Y 2013 Length of growing period over Africa: variability and trends from 30 years of NDVI time series *Remote Sens.* **5** 982–1000
- White M A, Thornton P E and Running S W 1997 A continental phenology model for monitoring vegetation responses to interannual climatic variability *Glob. Biogeochem. Cycles* **11** 217–34
- Xu C, McDowell N G, Fisher R A, Wei L, Sevanto S, Christoffersen B O and Middleton R S 2019 Increasing impacts of extreme droughts on vegetation productivity under climate change *Nat. Clim. Change* **9** 948–53
- Zscheischler J, Michalak A M, Schwalm C, Mahecha M D, Huntzinger D N, Reichstein M and Zeng N 2014 Impact of large-scale climate extremes on biospheric carbon fluxes: an intercomparison based on MsTMIP data *Glob. Biogeochem. Cycles* **28** 585–600
- Zscheischler J and Seneviratne S I 2017 Dependence of drivers affects risks associated with compound events *Sci. Adv.* **3** e1700263
- Zscheischler J, Westra S, van den Hurk B J J M, Seneviratne S I, Ward P J, Pitman A and Zhang X 2018 Future climate risk from compound events *Nat. Clim. Change* **8** 469–77